Bearing capacity of geosynthetic encased stone columns

Article *in* Geotextiles and Geomembranes · June 2013

DOI: 10.1016/j.geotexmem.2013.04.003

CITATIONS
184

READS
4,307

2 authors:

Mahmoud Ghazavi
Khaje Nasir Toosi University of Technology
83 PUBLICATIONS **1,847** CITATIONS
SEE PROFILE

Javad nazari afshar
Islamic Azad University ShahreQods Branch
11 PUBLICATIONS **331** CITATIONS
SEE PROFILE

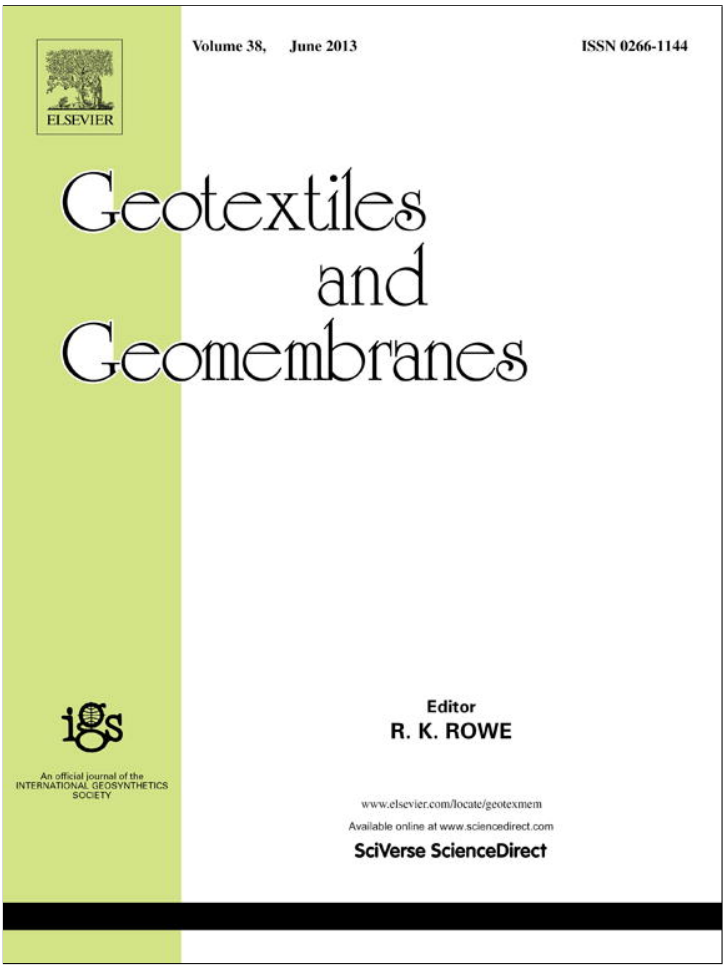

Geotextiles and Geomembranes 38 (2013) 26–36

Contents lists available at SciVerse ScienceDirect

Geotextiles and Geomembranes

journal homepage: www.elsevier.com/locate/geotexmem

Bearing capacity of geosynthetic encased stone columns

Mahmoud Ghazavi [a], Javad Nazari Afshar [b,*]

[a] Civil Engineering Department, K.N. Toosi University of Technology, Tehran, Iran
[b] Department of Civil Engineering, Shahr-e-Qods Branch, Islamic Azad University (IAU), Tehran, Iran

ARTICLE INFO

Article history:
Received 3 September 2012
Received in revised form
20 March 2013
Accepted 28 April 2013
Available online 7 June 2013

Keywords:
Stone column
Bulging
Ground improvement
Soil reinforcement
Geotextiles
Finite element analysis

ABSTRACT

The benefit of using stone columns in low strength soil has been proved as an efficient method to improve load-carrying characteristics of shallow footings. The stone column bearing capacity mainly depends on circumferential confinement providing by native soft soils. In this paper, some large body laboratory tests were performed on stone columns with diameters of 60, 80, and 100 mm and a length to diameter of 5. Both unreinforced and encased geotextile reinforced stone columns were tested. Vertical encased stone column (VESC) have been considered to investigate the effect of reinforcement on the footing load-carrying characteristics. The main objective of this research is to compare the effectiveness of vertical encapsulating of stone columns in the same conditions for various stone column diameters. In addition, tests on groups of stone columns with 60 mm diameter were carried out to investigate the effect of presence of neighboring columns on the reference loaded stone column. Results show that the stone column bearing capacity increases by using vertical reinforcing material. With increasing the length and strength of reinforcement in VESC, the stone column bearing capacity increases. In addition, the stress concentration ratio of columns also increases. Moreover, the lateral bulging decreases by using geotextiles. Numerical analysis based on finite element method (FEM) was also conducted to study scale effects on small stone columns tested and how to expand reinforcement effectiveness to large reinforced stone columns.

1. Introduction

In geotechnical engineering, the bearing capacity and settlement are two main criteria that control the design and performance of footings. In soft soils, the construction of structures such as a building, storage tanks, warehouse, etc, on weak soils usually involves excessive settlement or stability problems. To solve or reduce bearing capacity and settlement problems, soil improvement may be considered by using stone-columns. In addition, because of high permeability of stone column material, consolidation rate in soft clay increases.

One major constraint with stone columns is their failure under loading. Barksdale and Bachus (1983) described three failure types, which may occur for a stone column: bulging failure, shear failure, and punching failure. The bulging failure mechanism was described by Greenwood (1970), Vesic (1972), Hughes and Withers (1974), Datye and Nagaraju (1975), and Madhav et al. (1979). The shear failure mechanism was described by Madhav and Vitkar (1978), Wong (1975), and Barksdale and Bachus (1983). The punching failure mechanism was investigated by Aboshi et al. (1979).

Bouassida et al. (1995) proposed a new design method using a lower bound method within the framework of yield design theory for determination of bearing capacity of stone columns by taking three-dimensional effects of stone columns and surrounding native soil. Lee and Pande (1998) presented numerical modeling by using a homogenization technique. Abdelkrim and Buhan (2007) presented a new method for predicting the settlement of a foundation on stone column reinforced soil by use of an elastoplastic homogenization procedure. Deb (2008) and Deb et al. (2008) developed a mechanical model for prediction of behavior of soil reinforced with stone columns. They also considered the influence of unreinforced and geosynthetic reinforced granular bed constructed on a stone column head. In their study, stone columns, granular layer, and soft soil were idealized by stiffer Winkler springs, the Pasternak shear layer, and the Kelvin–Voigt, respectively.

Deb et al. (2011) have performed a series of laboratory tests to investigate the effect of sand bed reinforcement resting on stone columns. Wood et al. (2000) have performed a series of model tests on a clay bed reinforced with groups of stone columns to study the effect of reinforcement of the clay bed and deformation behavior of column groups under loading. Ambily et al. (2007) carried out a

* Corresponding author. Tel.: +98 21 46896461; fax: +98 21 46896001.
E-mail addresses: ghazavi_ma@kntu.ac.ir (M. Ghazavi), nazariafshar@yahoo.com (J. Nazari Afshar).

0266-1144/$ – see front matter © 2013 Elsevier Ltd. All rights reserved.
http://dx.doi.org/10.1016/j.geotexmem.2013.04.003

series of tests to study the behavior of single and group stone columns. They varied parameters such as spacing between stone columns, shear strength of soft clay on a 100 mm diameter column surrounded by soft clay with different undrained shear strength.

In very soft soils, unreinforced stone columns may not support significant loads due to low lateral confinement. In such situations, additional confinement can be provided by encasing the stone columns with geosynthetics. The encasement increases the bearing capacity, increases stiffness, and reduces lateral bulging of stone columns even in very soft soil. Van Impe (1989) proposed the idea of encasing the stone column by wrapping with geotextile. Murugesan and Rajagopal (2006), and Lo et al. (2010) have studied the performance of vertical encased stone columns (VESC) with geosynthetics using numerical models. Using the unit cell concept, Pulko et al. (2011) presented an analytical method for analysis of reinforced ground with unreinforced stone columns and vertically encased stone columns.

Murugesan and Rajagopal (2010) performed a series of single and group column load tests on stone columns installed using a displacement method, with and without encasement and using different geosynthetics. The results from the load tests indicated a positive effect of encasement on increasing the bearing capacity of VESC. Gniel and Bouazza (2010) performed laboratory tests to investigate the efficiency of new alternative method of encasement construction by compression test using different geogrid and stone column aggregates. Sivakumar et al. (2004) reported the efficiency of encasement by performing a series of triaxial tests on model sand columns in clay with and without vertical encasement with a varying penetration rate depth of column into clay. Wu and Hong (2009) presented a relationship for prediction of axial stress-strain behavior of encapsulated granular columns and verified this relationship by experimental triaxial test results on a reinforced sand specimen. Gniel and Bouazza (2008) and Wu et al. (2009) studied the effect of encasement on granular columns by triaxial testing and observed increasing strength and stiffness of granular columns due to increasing confining pressure provided by encapsulating reinforcement.

This paper reports the results of a series of large body tests on single and group of stone columns with various diameters. These tests involve OSCs and VESCs to investigate the effect of encased reinforcement, reinforcement type and length with different reinforcement materials.

2. Experimental investigation

2.1. Properties of materials

2.1.1. Clay and stone column material

Clay and crushed stone materials were used for current experimental investigations. The properties of the clay are listed in Table 1.

To determine the moisture content corresponding to 15 kPa undrained shear strength of the clay, a series of unconfined compressive strength (UCS) tests were carried out on cylindrical specimen with 38 mm diameter and 76 mm height. The results of variation of undrained shear strength with water content are depicted in Fig. 1. Water content of the clay was 28% (Fig. 1) and this amount was kept the same in all tests.

Crushed stone aggregates with particle sizes ranging 2–10 mm were used as stone column material and their properties are shown in Table 2. The particle size distribution for stone column and clay materials are depicted in Fig. 2.

2.1.2. Reinforcements

The selection of reinforcing material is important in laboratory tests from scale viewpoint. Reducing tensile strength of reinforcing material by proportion of physical scale of models helps to better represent the full-scale condition. In practice, reinforcement sleeves for vertical encasement of stone columns are produced with diameter of 40 cm–100 cm and tensile strengths of up to 400 kN/m and stiffness from 1000 to 4000 kN/m (e.g., Ringtrac® sleeves is a registered trademark of HUESKER Synthetic GmbH, Germany). For example, Araújo et al. (2009) reported the use of polyester woven geotextile to encase the stone column. The diameter of the geotextile casing and tensile strength, and stiffness of the geotextile were 0.4 m, 200 kN/m, and 2000 kN/m, respectively.

Table 1
Properties of clay.

Parameters	Value
Specific gravity	2.7
Liquid limit (%)	33
Plastic limit (%)	20
Plasticity index (%)	13
Optimum moisture content (%)	18
Maximum dry unit weight	16.8 kN/m^3
Bulk unit weight at 28% water content	19 kN/m^3
Undrained shear strength	15 kPa
Compression Index	0.17
USCS classification symbol	CL

According to the scaling laws proposed by Iai (1989), the relationship between prototype-scale reinforcement stiffness (J_P) and model-scale stiffness (J_m) can be calculated as $J_P = J_m\lambda^2$, where $1/\lambda$ is the model scale. In the current study, this is equal to 1/10. Two types of geotextile were used in the current study. The properties of geotextile material are listed in Table 3. The geotextile tensile strength properties were determined from standard wide width tension tests according to ASTM D 4595-05.

Table 4 presents a summary of the type and property of reinforcement material used by others for tests performed on VESC. In addition, geotextiles for this study had an ultimate tensile strength that falls in the range reported in Table 4.

In the current research work, large body stone columns with diameters of 60 mm, 80 mm, and 100 mm were reinforced using two types of nonwoven polypropylene geotextile. Vertically cylindrical reinforcement was made by overlapping a rectangular geotextile along the length of stone column. For all tests, an overlapping width of 15 mm was taken and overlapping seam was stuck with special polypropylene glue. Some control tension tests were performed on glued geotextile to ensure that the stuck seam has sufficient strength. The load deformation behavior observed from the tensile tests on different virgin and seamed geosynthetics is shown in Fig. 4. As seen, the glue for overlapping is satisfactory.

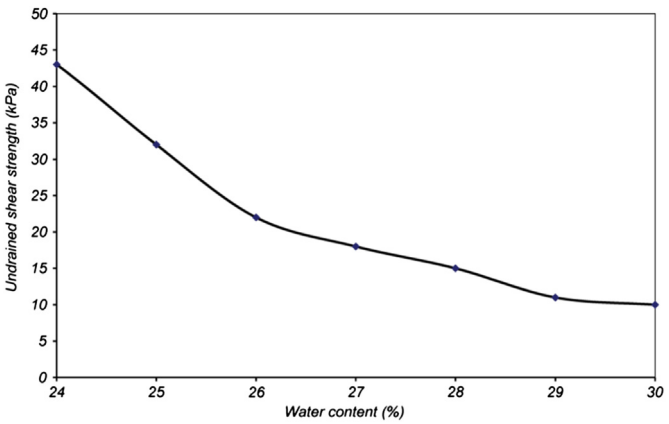

Fig. 1. Variation of undrained shear strength of clay with water content.

Table 2
Property of stone column material.

Parameters	Value
Specific gravity	2.7
Maximum dry unit weight	16.6 kN/m^3
Minimum dry unit weight	14.9 kN/m^3
Bulk unit weight for test at 68% relative density	16 kN/m^3
Internal friction angle (φ) at 68% relative density	46°
Uniformity coefficient (C_u)	2.16
Curvature coefficient (C_c)	1.15
Unified system classification	GP

2.2. Experimental setup and test program

A test setup was specifically designed for the current research work by the authors. This setup consists of a large test box with plan dimensions of 1.2 m × 1.2 m and 0.9 m height. This tank has a rigid loading frame for installing loading system and provides space for soft soil and stone column materials (Fig. 4a). The loading system is based on displacement control and speed of displacement of setup is controlled by a servomotor and related drive (Fig. 4a). The rotational movement of servomotor is changed to vertical displacement by special gearbox. A programmable logic controller (P.L.C) is used for data acquisition system and control of the setup. The test setup is connected to personal computer by software developed specifically for this setup.

In the current research, 18 tests were performed on single stone columns and 3 tests were carried out on groups of stone columns. For single stone column tests, a rigid steel plate with diameter of 200 mm and thickness of 30 mm was used as loading object (Fig. 4b). A miniature load cell was mounted in the center of the loading plate on the down side to measure the ratio of stress on stone column to that on the soft soil bed (Fig. 4b). It is noted that that some repeated tests were performed on stone columns to ensure that the results are repeatable and consistent. These tests showed good agreement.

The vertical displacement of the loading plate is measured by two L.V.D.T (linear variable differential transformer) displacement transducers. Single stone column tests were performed with a 200 mm diameter loading plate and different column diameters of 60, 80, and 100 mm. The ratio of L/D (length to diameter of the stone column) of 5 was used for all single stone column tests. This is because a minimum $L/D = 4$ is required for control of bulging failure mode (Barksdale and Bachus, 1983).

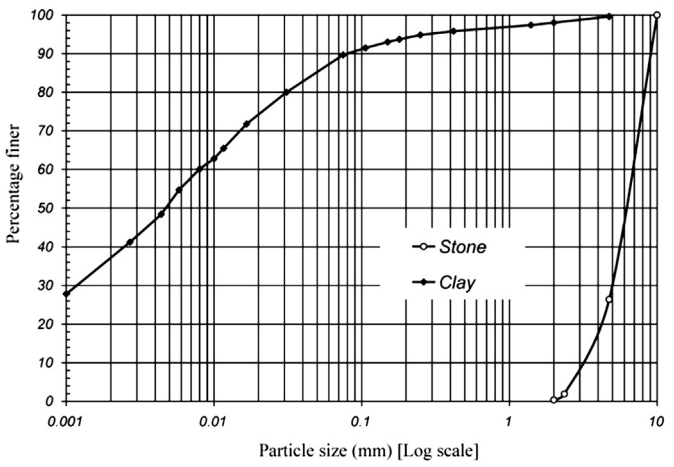

Fig. 2. Particle size distribution for stone column and clay materials.

Table 3
Properties of geosynthetics.

Parameters	Geotextile 1	Geotextile 2
Yarn material	Polypropylene	Polypropylene
Ultimate tensile strength (kN/m)	9	14
Strain at ultimate strength (%)	55	40
Secant stiffness at ultimate Strain (J) (kN/m)	16.36	35
Thickness (mm)	1	1.8
Mass (g/m^2)	140	180

It is known that the maximum bulging of stone column under loading usually occurs up to a depth of 1.5–2 times the diameter of stone column from the top of the column. Hence, only the top portion of the stone column needs more lateral confinement in order to reduce the bulging. Murugesan and Rajagopal (2006) carried out numerical analysis on performance of vertical encasement of stone columns and showed that the encasement beyond a depth equal to twice the diameter of the column does not lead to further performance improvement. Thus, the confinement at the top portion of the stone column may be adequate for performance improvement. To investigate this and also to ensure the validity of findings by Murugesan and Rajagopal (2006), in the current study, some tests were performed on single stone columns for which only half of their lengths were reinforced. For comparison, some tests were also performed on full encased stone columns. In all tests, the lengths of columns were 5 times their diameters thus half-lengths of encased stone columns were 2.5 times their diameters.

To study the effect of presence of adjacent columns, load tests were performed on 12 stone columns all had a diameter of 60 mm with center-to-center spacing of 150 mm equal to 2.5D where D is the column diameter. The column group was arranged with a triangle configuration as shown in Fig. 5. A circular plate of 260 mm diameter and 25 mm thickness was used as a loading plate. The diameter of the loading plate was selected so that it could just cover the central three stone columns at the center of the group of 12 stone columns (Fig. 5). A summary of these tests is presented in Table 5 in which in the test description column, L and 0.5L represent full length and half-length of encasement of VESC, respectively.

Table 4
Summary of type and property of reinforcement used by others.

Reference	Gniel and Bouazza. (2008)	Wu et al. (2009)	Murugesan and Rajagopal (2010)
Diameter of encased stone column (mm)	50.5	70	50, 75, and 100
Shear strength of reinforced soil (kPa)	5	–	2.5
Type of test	Model test on cylindrical cell with 550 mm height and 155 mm internal diameter	Triaxial compression test	Model test on tank with 120 cm × 120 cm dimension in plan
Reinforcing material	Fiberglass Aluminum	Geotextile, GT 1 Geotextile, GT 2 Geotextile, GT 3	Woven geotextile Nonwoven geotextile Soft grid-1 Soft grid-2
Ultimate tensile strength (kN/m)	8.4 6.8	3.84 6.20 8.77	20 6.8 2.5 1.5

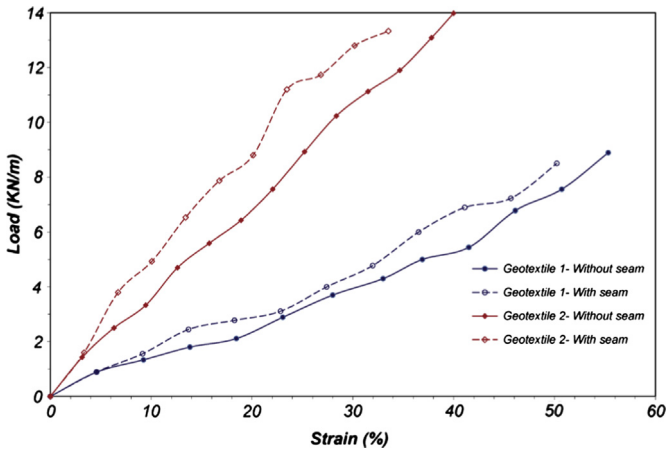

Fig. 3. Tensile load-strain behavior of geotextile samples with and without seam.

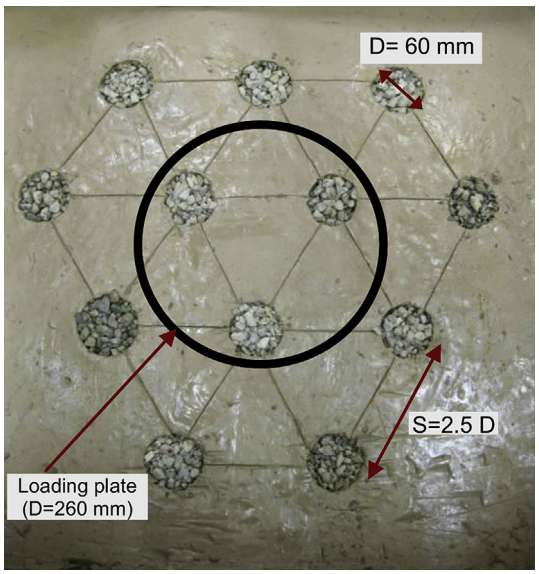

Fig. 5. Plan view of group tests arrangement.

2.3. Preparation of clay bed

Clay bed was prepared in a large test box with plan dimensions of 1.2 m × 1.2 m. The clay bed thicknesses of 300, 400, and 500 mm were used for stone columns with diameters of 60, 80, and 100 mm, respectively. The clay bed was prepared in layers each of which was 50 mm thick. To prepare the clay bed at a moisture content of 28% corresponding to 15 kPa undrained shear strength, initially natural water content of the clay was determined and the amount of additional water content was added to the clay to achieve 28% water content in a large plastic box. The surface of the box was sealed with a nylon sheet for five days to achieve uniform water content within the clayey soil mass. It was also used to prevent the clay moisture content loss by sealing the conjunction of floor and wall of test box. The inner face walls of the test box were coated by a thin layer of grease to reduce the friction between the clay and tank wall for each layer. The clay was placed in the tank with measured weight to reach a certain bulk unit weight of 19 kN/m^3. A uniform compaction effort was used on the entire surface of each clay layer to achieve a 5 cm height and uniform required density. A special tamper with 150 mm × 150 mm in plan and 10 kg mass was used for clay compaction. The drop height of the tamper was 200 mm. At the bottom of the tamper, five steel bars measuring 10 mm diameter and 20 mm length was used for kneading each clay layer. This helped to reduce left over air voids in the test bed and connect clay layers to each other.

The final surface of the clay bed was leveled and trimmed to have a proper thickness and surface in all tests. The same method was used in all tests for preparation of the clay bed. For all clay

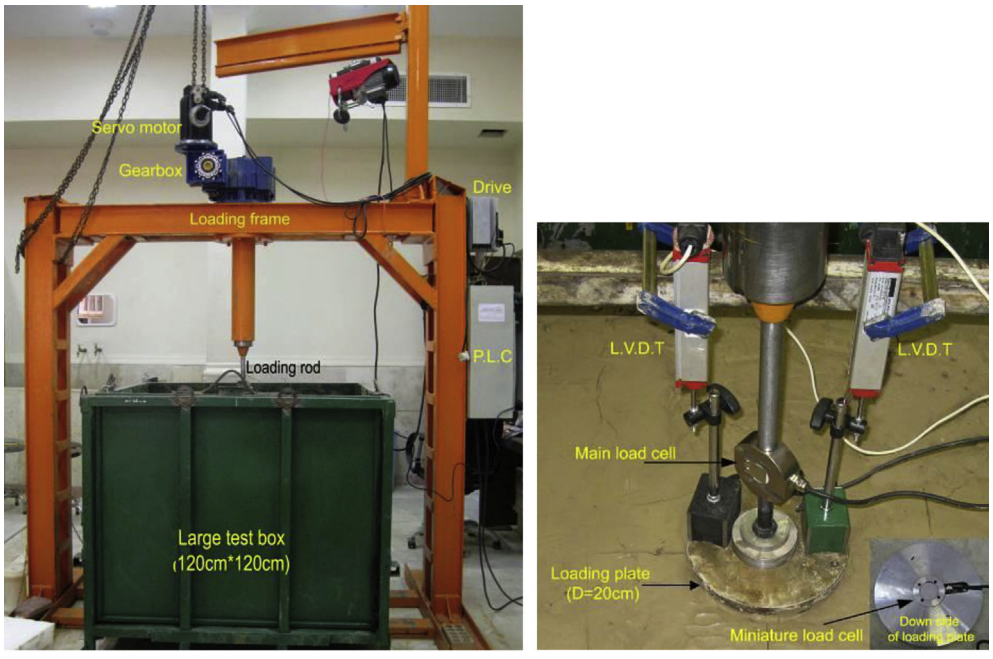

Fig. 4. Testing setup (a) loading frame and large test box (b) single stone column loading plate and data acquisition instruments.

Table 5
Outline of load tests on stone columns.

Test type	Test description	Reinforcing material	Diameter of stone column (mm)			Total number of tests
			60	80	100	
Single stone column	Clay bed	–	✓	✓	✓	3
	OSC	–	✓	✓	✓	3
	VESC (L)	Geotextile 1	✓	✓	✓	3
	VESC (L)	Geotextile 2	✓	✓	✓	3
	VESC (0.5L)	Geotextile 1	✓	✓	✓	3
	VESC (0.5L)	Geotextile 2	✓	✓	✓	3
Group of stone columns	Clay bed	–	✓	–	–	1
	OSC	–	✓	–	–	1
	VESC (L)	Geotextile 1	✓	–	–	1

(Note: L and 0.5L denote full length and half-length of reinforcement, respectively. OSC: Ordinary stone column – VESC: Vertical encased stone column).

layers, the water content profile was determined at 10 cm intervals to ensure that the moisture content in the clay was kept the same. In all tests, care was taken to maintain water content of clay bed layers at desired level. It was checked in all tests that a variation of moisture content was less than 1% in the clay bed. To further ensure that the undrained shear strength remained the same and for controlling the undrained shear strength of the clayey soil, after tests, 3 unconfined compression tests were performed on the specimens that were taken from different depths of the clay bed around the stone column. Again, unconfined compression tests showed a good agreement between the water content of 28% and corresponding 15 kPa undrained shear strength of the clay.

2.4. Construction of reinforced and unreinforced stone column

In all tests (OSC and VESC), stone columns with diameters of 60, 80, and 100 mm for single or group tests were constructed by the replacement method. All columns for single or group tests were constructed at center of large test box (Fig. 4b and Fig. 5). The plan dimension of tank was selected such that results of test would not be affected by boundaries of the tank. Thin walled, open-ended seamless steel pipes with outer diameters of 60, 80, and 100 mm and wall thickness of 2 mm were used for stone column construction. For all tests, both inner and outer surfaces of the steel pipes were coated by thin layer of oil to ease penetration and withdrawal without any significant disturbance to the surrounding soil. The steel pipe was then pushed into the clay to reach the bottom. Three different helical steel augers were designed and used for construction of stone columns. This diameter was slightly less than the inner diameter of the steel pipes. The clay inside the pipe was excavated by using a helical auger at maximum height of 50 mm at a time to make the clay removal easy. This ensured that no suction effects occurred. The steel pipe was pulled out slowly after removing clay within the pipe. Therefore, care was taken to prevent disturbance between the pipe and skin of the hole.

For VESC tests, a circular wooden rod with 95, 75, and 55 mm diameters were prepared and vertical reinforcement layer was positioned in the excavated hole. The quantity of stone aggregates required to form the stone column was calculated based on required bulk unit weight of 16 kN/m^3 and charged into the hole in layers of half column diameter (0.5D). To achieve a uniform density, compaction was done with a 2 kg mass using a circular steel tamper with 20 mm diameter. The free drop height was 100 mm with 15 blows. This light compaction effort was chosen such that no significant lateral bulging occurred during column construction or disturbance of the surrounding soft clay. Granular materials of stone columns sustain higher stress than the clay bed. This may lead to the breakage of stone granular materials under loading. For solving this problem, high quality of granular material was selected so that breakage of the stone column material could not occur under high stress level due to the column loading and light stress induced due to compaction. Enough amount of stone column material was prepared to keep uniformity in tests and new stone column material used in each new test, not the material used for the previous tests. A visual control always made on the column material to ensure that no breakage occurred upon the column loading or compaction loading.

3. Test procedure

The test procedure involves application of the load and determination of load-displacement behavior of the clay treated with stone columns. Following installation of the stone column, the load was applied using a plate oriented in the center of the column and clay bed. The load was applied on the plate with a constant displacement rate of 1 mm/min. The loading of each test was continued to a displacement of up to 50 mm.

4. Results and discussion

4.1. Deformation and failure mode

After completion of some tests, the deformed shapes of single and group stone columns in OSC and VESC tests were captured by filling paste of plaster of Paris in stone column and dented place of loading plate (Fig. 6). In all tests on single stone columns, it was observed that the bulging failure mode governed. The bulging failure occurred at a depth of D to 2D from the stone column head as seen in Fig. 6(a). In addition, in all single VESC tests, bulging failure occurred but the size of bulging was smaller than that observed in OSC tests. The failure mode observed in stone column groups was a combination of bulging and lateral deflection of stone columns. As observed in tests, the lateral displacement of columns was mostly outward from the plate edge and was greater than that toward the plate center. The deformations of group tests were similar to the deformation of group of stone columns observed by Wood et al. (2000). In single stone column tests, because of central location of columns under the loading plate, the stress in the stone column and around the clay bed were uniform and the shape of bulging was axisymmetric. However, in the group of stone column tests, because columns were not located at the center of loading plate

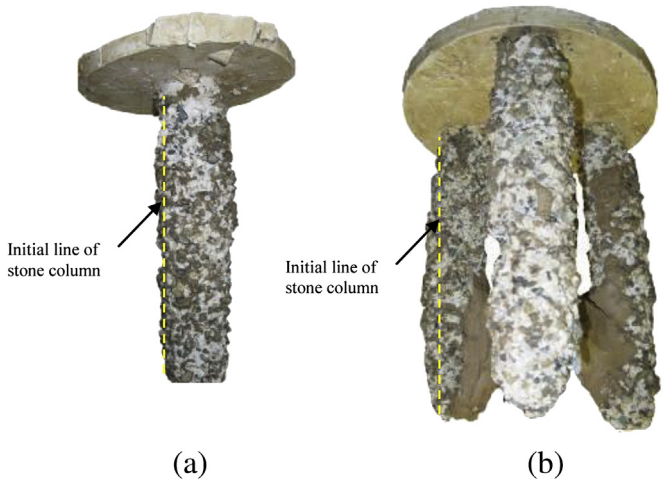

Fig. 6. Shape of stone column after (a) single test (b) group test.

(Fig. 5), the stress due to loading around stone columns were not the same. The periphery stress around the stone column decreases to outward from the plate edge. Therefore, the columns move to outward from the plate edge and deformation of stone columns in the group tests were combinations of bulging and outward lateral deflection. As a result, bending in columns was observed outward of the plate, as shown in Fig. 6(b). In addition, the lateral deflection and bulging of stone column groups were reduced in VESCs tests compared with groups of OSCs.

4.2. Load-settlement behavior

Fig. 7a–c illustrate the load-settlement behavior of isolated stone columns (OSC's and VESC's) with diameters of 60, 80, and 100 mm. As seen, in all OSC's and VESC's, there exists an increase in the ultimate load-carrying capacity of the soft soil. In addition, the ultimate capacities of columns (OSC's and VESC's) increase with increasing the stone column diameter. Moreover, geosynthetic material used for vertical encasement increases the stone column ultimate capacities. Results of single VESCs for two types of geotextile material and different strength are also shown. Additionally, load-settlement characteristics of VESCs with various lengths for vertical encasement are presented. From Fig. 7a–c, it is obvious that vertical encasement provides greater stone column ultimate capacity and stiffness. In addition, such reinforcement reduces the lateral bulging of stone columns. Moreover, by increasing the ultimate tensile strength of encasement material, the ultimate bearing capacity of VESCs increases for both full and half-length stone column encasement compared with that of OSC's. As also seen, full-length encasement of the stone column is more efficient than half-length encasement for VESCs. However, the efficiency of half-length encasement of stone columns increases with increasing the stone column diameter from 60 to 80 mm. In all tests on stone columns with different diameters of 60, 80, and 100 mm, the diameter of loading plate was 200 mm. After completion of tests, the clay around the stone column was carefully cut in the vertical direction and the size of maximum lateral bulging was measured. Measured results show that ratio of the maximum bulging to initial diameter of the column increased by increasing the stone column diameter. This means that by increasing the diameter of columns, the radial strain of encasement increased. Fig. 3 shows that the mobilized tensile stress in geotextile materials increases by increasing the strain. Thus, by increasing the diameter of the columns, the mobilized tensile strength and lateral confinement of encasements on columns increase. As a result, the column efficiency increases for half-length encasement by increasing the stone column diameter.

Fig. 8 shows results of tests performed on a group of stone columns. The column configuration is shown in Fig. 5. The group tests consist of OSCs and VESCs. Vertical reinforcement in group tests was provided using geotextile 1. As seen, the use of group of OSC's improves load-settlement response of reinforced soft soil. In addition, the use of VESCs in group of stone columns increases the ultimate bearing capacity.

4.3. Improved load ratio

To determine the efficiency of stone columns from the viewpoint of the ultimate bearing capacity, the load ratio ($L.R$) parameter is defined as:

$$L.R = \frac{\text{Ultimate load obtained from stone column reinforced soil}}{\text{Ultimate load obtained from soft soil with no stone column}} \quad (1)$$

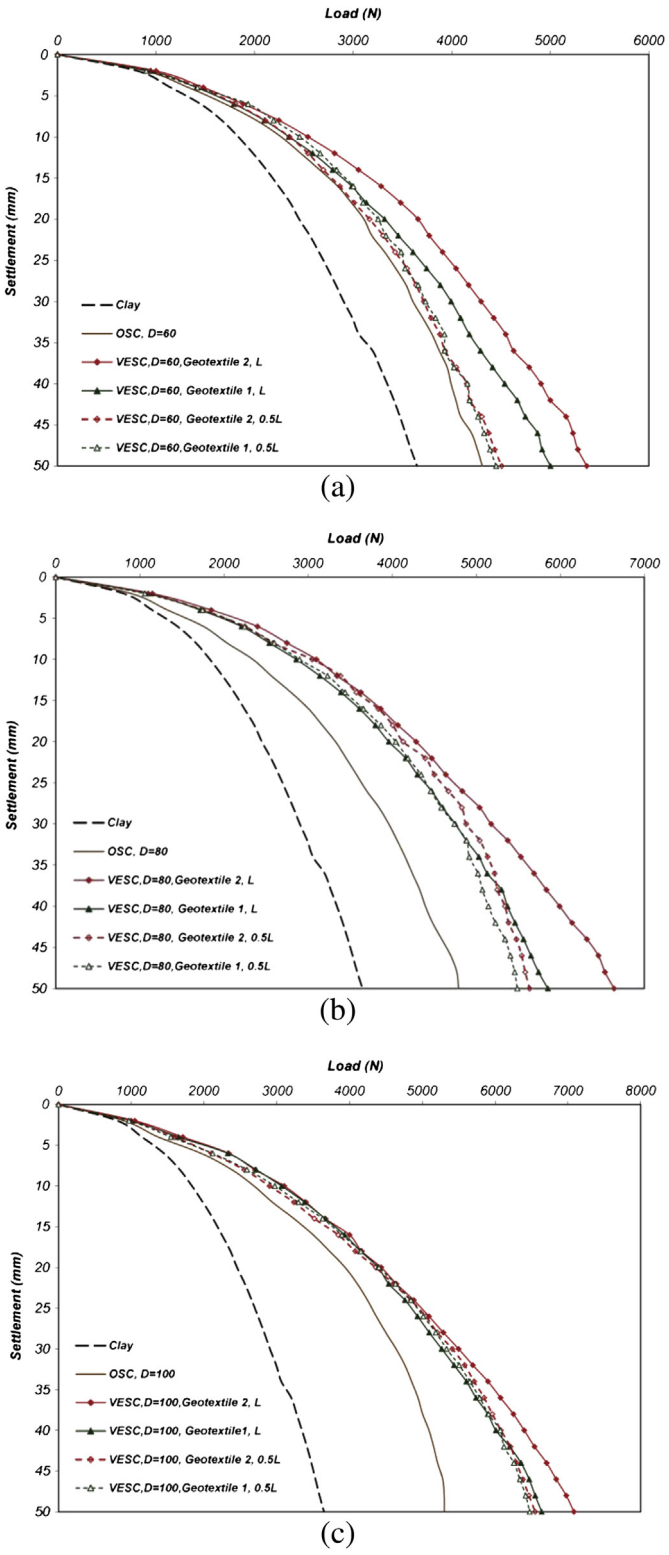

Fig. 7. Load-settlement variation of single stone columns with diameters: (a) 60 mm (b) 80 mm (c) 100 mm.

Fig. 9a–c shows the $L.R$ variation with the settlement for stone columns having diameters of 60 mm, 80 mm, and 100 mm with different tensile strength for reinforcement materials. As seen, the $L.R$ varies in the range of 1.18–1.48, 1.32–1.82, and 1.48–1.94 for stone columns having diameters of 60 mm, 80 mm, and 100 mm,

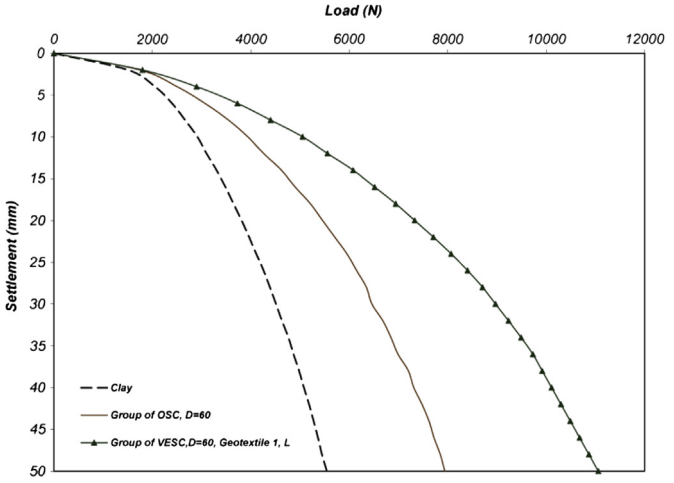

Fig. 8. Load-settlement variation of stone column groups with 60 mm diameter.

respectively. The minimum *L.R* is for OSCs and the maximum *L.R* is for full-length encasement of VESCs with stronger geotextile used in the current study. In addition, the *L.R* value increases with increasing the length and tensile strength of reinforcing material in VESCs. This is because reinforcement material provides lateral confinement for columns and reduces bulging. Fig. 9a–c also show that with increasing the loading up to a settlement of about 20 mm, the value of *L.R* increases and by increasing settlement over than 20 mm, the value of *L.R* decreases in OSCs with different diameters due to the occurrence of bulging and reaching the column to its final strength. The value of *L.R* increases for VESCs with half-length reinforcement with increasing the column diameters from 60 mm to 100 mm.

Fig. 10 shows the variation of *L.R* with increasing loading plate displacement. As seen, the use of group stone columns increases the ultimate load and the *L.R* values vary in the range of 1.42–2.02. The minimum *L.R* value is for group of OSCs and the maximum *L.R* is for full-length encasement of groups of VESC's.

4.4. Stress concentration ratio

The external load is distributed between stone columns and soft soil in terms of the ratio of the column stiffness to that of the soft soil. Since the column stiffness is greater than that of the soft soil, the stresses on the columns are greater than those in the surrounding soft soil. In the literature, the ratio of stress in stone columns to stress in soft surrounding soil is defined as stress concentration ratio (SCR) and denoted by *n*. Fig. 11a–c show the SCR variation with the settlement for OSCs and VESCs with various diameters of 60 mm, 80 mm, and 100 mm. As seen, the SCR value is not constant for all stone columns and varies with increasing the column settlement. Fig. 11a–c also show that the ultimate value of SCR varies in the range of 3.2–6.3, 3–5.6, and 3.1–5.1 for columns with diameters of 60 mm, 80 mm, and 100 mm, respectively. The minimum and maximum value of SCR is for OSCs and full length reinforced VESCs, respectively. As also seen, by increasing the length and tensile strength of reinforcement material, the SCR value increases due to increasing the stone column stiffness. The SCR value increases for settlement up to 3 mm and then decreases with increasing the settlement and then approaches almost a constant value. In OSCs, at the first stage of loading up to 3 mm displacement, the stone column moves downward and causes rearrangement of stone column grains. This increases slightly the column material densification. This leads to mechanical

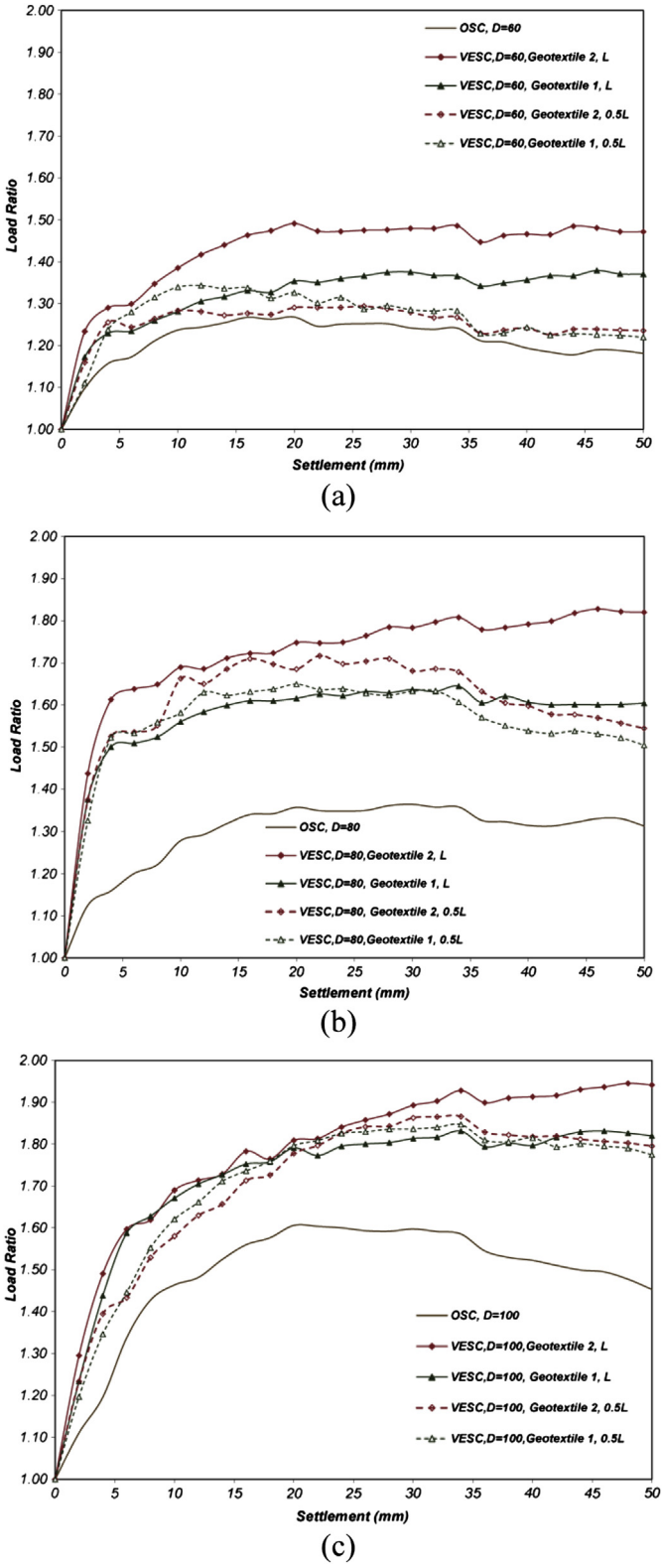

Fig. 9. Variation of load ratio versus settlement for various stone columns with diameters of: (a) 60 mm (b) 80 mm (c) 100 mm.

interlocking between grains. With increasing the load and settlement, granular material tends to move laterally toward the surrounding soft soil. This causes a gradual transfer of the load to the soft soil. As a result, the SCR decreases. In VESCs, the reinforcing

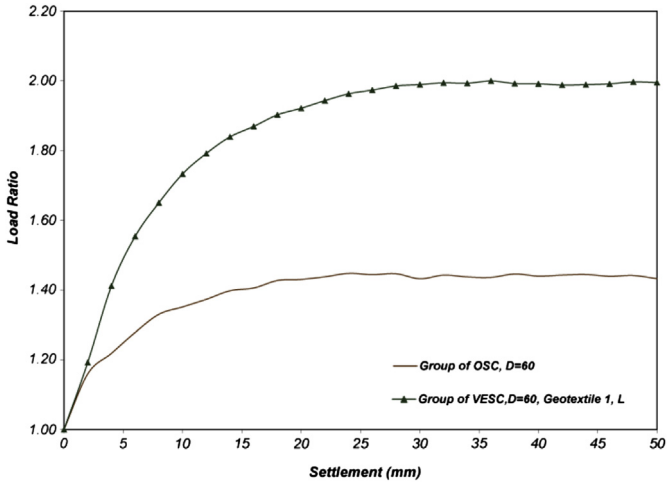

Fig. 10. Variation of load ratio versus settlement in-group stone columns with 60 mm diameter.

material provides additional lateral confinement. Thus, the SCR value decreases slightly compared with OSCs. As seen in Fig. 11a–c, with increasing the stone column diameter, the benefit of encasement decreases. Thus, the SCR value of reinforced columns with smaller diameters is higher than that of columns with larger diameters for the same encasement. This may be attributed to the mobilization of higher confining stresses in smaller diameter of stone columns.

5. Scale effects for experiments

Results of this study were obtained from small-scale model tests. Modeling of stone columns in small-scale gives an opportunity to make comprehensive study about reinforcement of columns of different shapes and materials. To extend the results from small-scale tests to real scale design, it is necessary to study scale effects of models in experiments. However, to study scale effects of model geometry and reinforcing material stiffness (J), some selected results of experimental tests are compared with results of FEM analysis carried out using PLAXIS software. The constructed numerical soil-column system behavior was validated using experimental data obtained for two single OSC and VESC tests. Properties of clay and stone are shown in Table 6. It is noted that the values presented in Table 6 were measured in the laboratory.

In the present paper, an axisymmetric finite element analysis was carried out on isolated and groups of stone columns. The Mohr–Coulomb failure criterion was assumed to govern the failure stage of the clay and stone column material. A linear-elastic behavior for geosynthetic material was assumed. In the finite element discretization, 6-noded triangular elements with geometry and boundary conditions as introduced in tests were used. All analyses were performed by applying displacement increments. Fig. 12 compares the results obtained from the laboratory model tests and FEM analysis. As seen, this comparison is satisfactory.

Table 7 compares experimental and numerical values of $L.R$ for single VESCs reinforced by Geotextile2 and group of VESC's reinforced by Geotextile1. As seen, there is very good agreement between experimental and numerical results.

To investigate the effect of reinforcement, numerical analysis carried out on vertical encased single stone columns with diameter of 0.6 m, 0.8 m, and 1 m all with L/D (length to diameter of the stone column) ratio of 5. To study the effect of encasement for group of stone columns, two configurations were used for stone columns

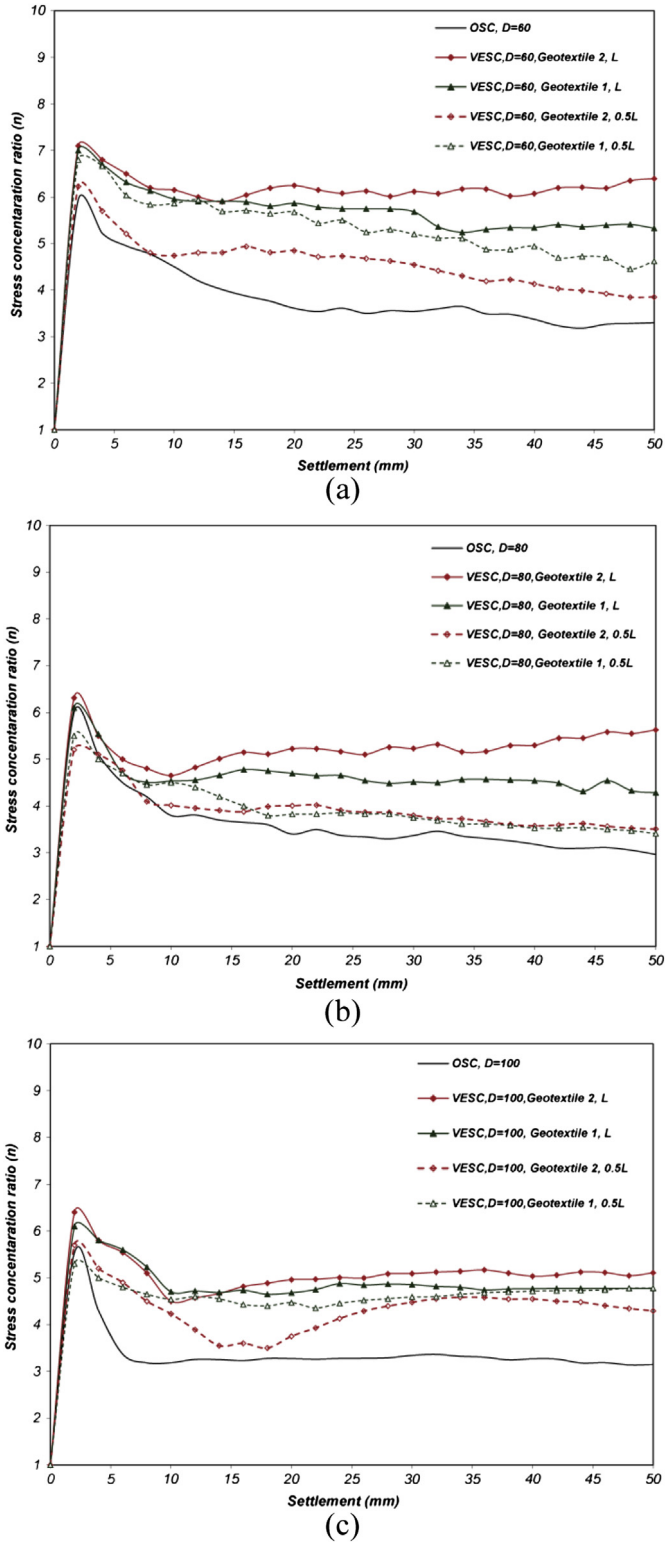

Fig. 11. Variation of stress concentration ratio versus settlement for stone columns with diameters of: (a) 60 mm (b) 80 mm (c) 100 mm.

with diameters of 0.6 m, 0.8 m, and 1 m. For this study, also $L/D = 5$ was used. As shown in Fig. 13, two groups of 3 and 7 stone columns with triangular configuration and $S = 2.5D$ were considered. In all analyses on stone column groups, the ratio of area replacement was chosen to be 16%. For these analyses, material properties are the

Table 6
Properties of materials used for validation of PLAXIS.

Parameters	Properties		
	Clay	Stone	Geotextile
Modulus of elasticity (kPa)	600	40,000	–
Poisson's ratio (μ)	0.47	0.3	–
Shear strength (kPa)	15	0	–
Internal friction angle (φ)	0	46°	–
Secant stiffness (kN/m)	–	–	35

Table 7
Comparison of load ratio (*L.R*) obtained from tests and numerical analysis.

Type of tests on VESC	Diameter of stone column (mm)	Load ratio (*L.R*)	
		Experiment	F.E.M (Plaxis)
Single	60	1.47	1.56
	80	1.82	1.85
	100	1.94	2.09
Group	60	2	1.89

same as presented in Table 6. For analysis of group of stone columns, an axisymmetric configuration was used such that the group of stone columns were replaced by a ring of stone column having an equivalent thickness (Fig. 13). Mitchell and Huber (1985), Elshazly et al. (2006), and Ambily et al. (2007) used similar modeling simulation.

In numerical analysis, the group of 3 columns (Fig.13b) is replaced with a ring which has identical material volume equal to the summation of material volumes in all 3 stone columns. In Fig. 13a, the ring passes the centers of 3 stone columns. The cross section of this ring is equal to the summation of cross sections of all 3 stone columns in the group. For 7 stone columns in the group, the equivalent ring passes through the centers of all 6 columns located at the periphery of the group (Fig. 13b). The thickness of this ring is determined such that the area of the ring becomes equal to the summation of cross sections of all 6 periphery stone columns (Fig. 13a).

For reinforcement of equivalent rings in Fig. 13a and b, the reinforcement is assumed to cover both internal and external vertical sides of the ring. Thus, the whole area of reinforcement around two vertical sides of the equivalent ring is greater than the summation of real areas of reinforcement around peripheries of all stone columns. To compensate this, in numerical analysis, the stiffness (J) of the vertical reinforcement in equivalent ring is reduced by the ratio of the summation of the area of reinforcement in the equivalent ring divided by the summation of areas of reinforcement around all peripheries of all columns in the group. It is noted that in 7 column group, the central column is directly modeled in numerical analysis and is not considered in modeling the equivalent ring (Fig. 13b). Thus, its real stiffness is not reduced and comes directly into numerical analyses.

Three different stiffnesses (J) were selected in numerical analysis to investigate the effect of reinforcement stiffness. In tests on

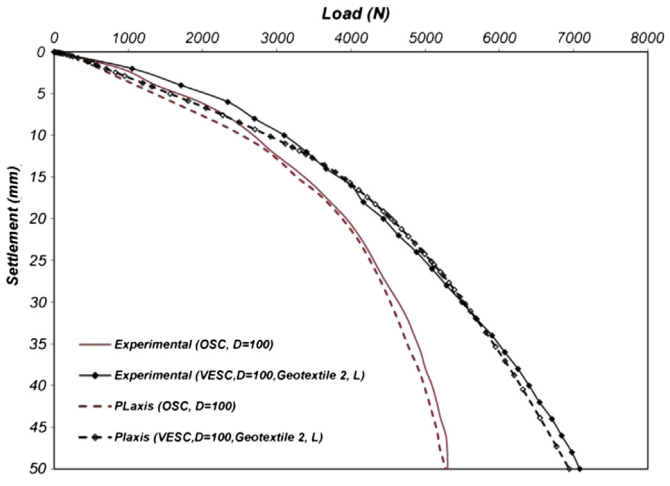

Fig. 12. Validation of Plaxis.

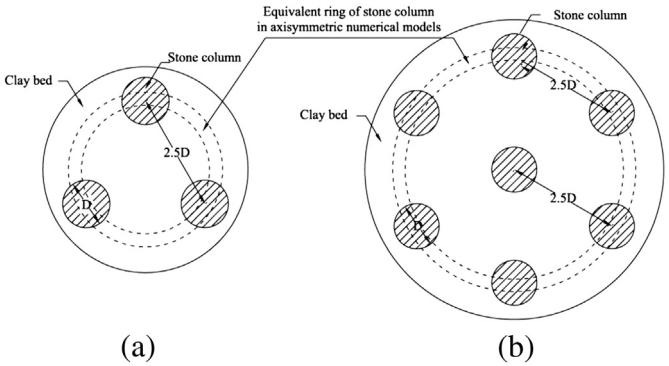

Fig. 13. Group arrangement for analysis (a) 3 stone columns (b) 7 stone columns.

small scale columns, $J = 35$ kN/m was used for the stiffness of Geotextile2. In numerical analyses of large-scale columns, $J = 1000$ kN/m and $J = 5000$ kN/m were used. Such values were used by Murugesan and Rajagopal (2006). In group of stone columns, the stiffness of encasement in the equivalent ring was reduced by the ratio mentioned above, but the stiffness of encasement in central column (Fig. 13b) was not reduced.

Table 8 presents *L.R* values obtained from FEM analysis for reinforced stone columns. As seen, the *L.R* values for vertically encased single and group of stone columns with 0.6 m diameter and for $J = 35$ kN/m have a very good agreement with *L.R* values obtained from tests performed on small-scale tests with the same reinforcement material (Fig. 9a–c and Fig. 10). Hence, it is inferred that the results of small-scale tests may be used to study the performance of vertically encased real scale stone columns. As also seen in Table 8, the *L.R* value for single stone columns increases by increasing the diameter of columns and increasing stiffness (J) of reinforcing material. As seen in Table 8, the *L.R* value in two configurations of group of stone columns increases by increasing the

Table 8
Plaxis results of influence of reinforcement stiffness on *L.R* of large-scale stone columns.

Type of VESC	Stiffness of reinforcement, J (kN/m)	Load ratio (*L.R*)		
		Diameter of stone column (m)		
		0.6	0.8	1
Single	35	1.4	1.7	2
	1000	2.9	3.2	3.6
	5000	5.8	6.7	7.4
Group (3 stone column)	35	1.8	1.7	1.6
	1000	2.6	2.2	2
	5000	5.3	3.8	3.5
Group (7 stone column)	35	1.8	1.8	1.7
	1000	2.8	2.3	2.2
	5000	5.8	4.2	3.7

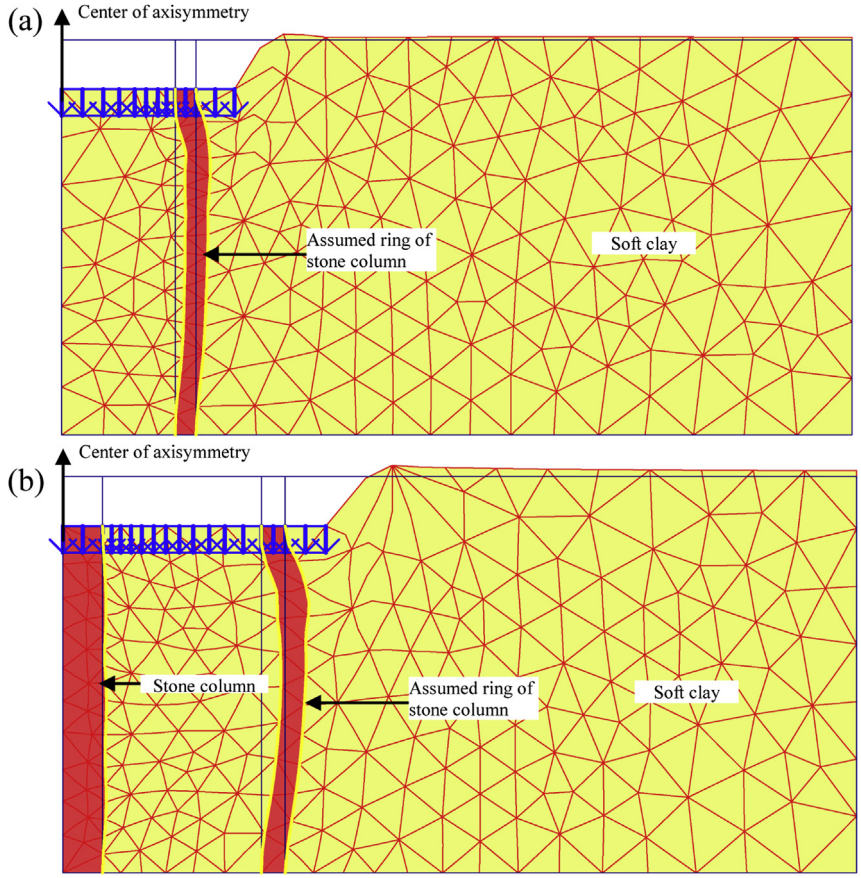

Fig. 14. Deformed mesh for group analysis of (a) 3 stone columns (b) 7 stone columns.

stiffness (J) of reinforcing material. However, the $L.R$ value decreases by increasing the diameter of stone columns. In 7 stone column group, the $L.R$ values are greater than that of 3 stone column group by increasing the stiffness of reinforcement and diameter of stone columns. It should be mentioned that the area replacement ratio in two different arrangements of stone columns was equal to 16%.

Fig. 14 depicts the deformed shape of group of VESC. As seen in group with 3 columns, the governing deformation of columns consists of slightly bulging and lateral deformation is major form of deformation (Fig. 14a). However, in group with 7 stone columns, major deformation is bulging for central columns and lateral deformation for periphery stone columns (Fig. 14b). In 7 column groups, the deformation mode on central columns is bulging which in turn causes to increase the performance of encasement in comparison to periphery columns. In 7 column groups, greater $L.R$ values are achieved compared with those values in 3 column group by using the same area replacement ratio. The lateral deformation of columns reduces the efficiency of vertical reinforcement. This is because the reinforcement has no bending stiffness and thus the $L.R$ value in single stone columns is greater than that in group of VESC's.

6. Conclusions

In this investigation, large body laboratory tests have been performed on single and group stone columns with diameters of 60 mm, 80 mm, and 100 mm. VESCs with different lengths and reinforcing material were used in tests and the results were compared with those obtained from tests on OSCs. Based on results from experiments on single and group of stone columns, the following concluding remarks may be extracted:

1. Bulging failure mode governs single stone columns. The bulging failure usually occurs at a depth of D to $2D$ from the stone column head. The failure mode in stone column group was a combination of bulging and lateral deformation.
2. The ultimate load carried by soft soil increases by using OSCs. The ultimate load and stiffness of the treated soil can be further increase by the use of vertical (VESCs) reinforcing material.
3. The lateral bulging amount decreases in VESCs compared with OSCs due to additional lateral confinement provided by geosynthetics material.
4. With increasing the length and strength of reinforcing encasement, the ultimate capacity and stiffness of stone columns increase.
5. Tests on group of stone columns have shown that the ultimate capacity of VESCs is greater than that of group of OSCs.
6. The value of stress concentration ratio in VESCs is higher than that in OSCs. This ratio decreases with increasing the settlement and stone column diameter.
7. Numerical analysis results on group of VESC's have shown that value of the $L.R$ with the same area replacement ratio depends on geometrical configuration of columns.

References

Abdelkrim, M., De Buhan, P., 2007. An elastoplastic homogenization procedure for predicting the settlement of a foundation on a soil reinforced by columns. European Journal of Mechanics A/Solids 26, 736–757.

Aboshi, H., Ichimoto, E., Harada, K., Emoki, M., 1979. The composer – a method to improve the characteristics of soft clays by inclusion of large diameter sand columns. In: Proceedings of International Conference on Soil Reinforcement, E.N.P.C, 1, Paris, pp. 211–216.

Ambily, A.P., Gandhi, S.R., 2007. Behavior of stone columns based on experimental and FEM analysis. Journal of Geotechnical and Geoenvironmental Engineering, ASCE 133 (4), 405–415.

Araújo, G.L.S., Palmeira, E.M., da Cunha, R.P., 2009. Geosynthetic encased columns in a tropical collapsible porous clay. In: Proceedings of the 17th International Conference on Soil Mechanics and Geotechnical Engineering, pp. 889–892.

Barksdale, R.D., Bachus, R.C., 1983. Design and Construction of Stone Column. Report No.FHWA/RD-83/026. National Technical Information Service, Springfield, Virginia.

Bouassida, M., De Buhan, P., Dormieux, L., 1995. Bearing capacity of a foundation resting on a soil reinforced by a group of columns. Geotechnique 45 (1), 25–34.

Datye, K.R., Nagaraju, S.S., 1975. Installation and testing of rammed stone columns. In: Proceedings of IGS Specialty Session, 5th Asian Regional Conference on Soil Mechanic and Foundation Engineering, Bangalore, India, pp. 101–104.

Deb, K., 2008. Modeling of granular bed-stone column-improved soft soil. International Journal for Numerical and Analytical Methods in Geomechanics 32, 1267–1288.

Deb, K., Chandra, S., Basudhar, P.K., 2008. Response of multilayer geosynthetic-reinforced bed resting on soft soil with stone columns. Computers and Geotechnics 35, 323–330.

Deb, K., Samadhiya, N.K., Babasaheb Namdeo, J., 2011. Laboratory model studies on unreinforced and geogrid-reinforced sand bed over stone column-improved soft clay. Geotextiles and Geomembranes 29 (2), 190–196.

Elshazly, H., Hafez, D., Mosaad, M., 2006. Back calculating vibro-installation stresses in stone columns reinforced grounds. Journal of Ground Improvement 10 (2), 47–53.

Gniel, J., Bouazza, A., 2008. Improvement of soft soils using geogrid encased stone columns. Geotextiles and Geomembranes 27 (3), 167–175.

Gniel, J., Bouazza, A., 2010. Construction of geogrid encased stone columns: a new proposal based on laboratory testing. Geotextiles and Geomembranes 28, 108–118.

Greenwood, D.A., 1970. Mechanical improvement of soils below ground surface. In: Proceedings of Ground Improvement Conference. Institute of Civil Engineering, pp. 9–29.

Hughes, J.M.O., Withers, N.J., 1974. Reinforcing of soft cohesive soils with stone columns. Ground Engineering 7 (3), 42–49.

Iai, S., 1989. Similitude for shaking table tests on soil-structure fluid models in 1g gravitational field. Soils and Foundations 29 (1), 105–118.

Lee, S., Pande, G.N., 1998. Analysis of stone column reinforced foundations. International Journal for Numerical and Analytical Methods in Geomechanics 22, 1001–1020.

Lo, S.R., Zhang, R., Mak, J., 2010. Geosynthetic-encased stone columns in soft clay: a numerical study. Geotextiles and Geomembranes 28 (3), 292–302.

Madhav, M.R., Vitkar, R.P., 1978. Strip footing on weak clay stabilized with a granular trench or pile. Canadian Geotechnical Journal 15 (4), 605–609.

Madhav, M.R., Iyengar, N.G.R., Vitkar, R.P., Nandia, A., 1979. Increased bearing capacity and reduced settlements due to inclusions in soil. In: Proceedings of International Conference on Soil Reinforcement: Reinforced and Other Techniques, pp. 239–333.

Mitchell, J.K., Huber, T.R., 1985. Performance of a stone column foundation. Journal of Geotechnical Engineering, ASCE 111 (2), 205–223.

Murugesan, S., Rajagopal, K., 2006. Geosynthetic-encased stone columns: numerical evaluation. Geotextiles and Geomembranes 24, 349–358.

Murugesan, S., Rajagopal, K., 2010. Studies on the behavior of single and group of geosynthetic encased stone columns. Journal of Geotechnical and Geoenvironmental Engineering, ASCE 136 (1), 129–139.

Pulko, B., Majes, B., Logar, J., 2011. Geosynthetic-encased stone columns: analytical calculation model. Geotextiles and Geomembranes 29, 29–39.

Sivakumar, V., McKelvey, D., Graham, J., Hughes, D., 2004. Triaxial test on model sand columns in clay. Canadian Geotechnical Journal 41, 299–312.

Van Impe, W.F., 1989. Soil Improvement Techniques and Their Evolution. Balkema, Rotterdam, The Netherlands.

Vesic, A.S., 1972. Expansion of cavities in infinite soil mass. Journal of Soil Mechanics and Foundation Engineering Division, ASCE 98 (SM3), 265–290.

Wong, H.Y., 1975. Vibroflotation – its effect on weak cohesive soils. Civil Engineering (London) 82, 44–76.

Wood, D.M., HU, W., Nash, D.F.T., 2000. Group effects in stone column foundation: model tests. Geotechnique 50 (6), 689–698.

Wu, C.S., Hong, Y.S., Lin, H.C., 2009. Axial stress–strain relation of encapsulated granular column. Computers and Geotechnics 36, 226–240.

Wu, C.S., Hong, Y.S., 2009. Laboratory tests on geosynthetic encapsulated sand columns. Geotextiles and Geomembranes 27 (2), 107–120.